PAPER • OPEN ACCESS

The effect of low temperature atmospheric nitrogen plasma on MC3T3-E1 preosteoblast proliferation and differentiation *in vitro*

IOP ebooks™

Bringing you innovative digital publishing with leading voices to create your essential collection of books in STEM research.

Start exploring the collection - download the first chapter of every title for free.

The effect of low temperature atmospheric nitrogen plasma on MC3T3-E1 preosteoblast proliferation and differentiation *in vitro*

Agata Przekora[1] **, Joanna Pawlat**[2]**, Piotr Terebun**[2]**, David Duday**[3]**, Cristina Canal**[4]**, Sophie Hermans**[5] **, Maïté Audemar**[5]**, Cédric Labay**[4]**, Jean-Sébastien Thomann**[3] **and Grazyna Ginalska**[1]

[1] Chair and Department of Biochemistry and Biotechnology, Medical University of Lublin, Chodzki 1 Street, 20-093 Lublin, Poland
[2] Institiute of Electrical Engineering and Electrotechnologies, Lublin University of Technology, Nadbystrzycka 38a, 20-618 Lublin, Poland
[3] Material Research and Technology (MRT) Department, Luxembourg Institute of Science and Technology (LIST), 41, rue du Brill, L-4422 Belvaux, Luxembourg
[4] Biomaterials, Biomechanics and Tissue Engineering Group, Department of Materials Science and Metallurgy, Universitat Politècnica de Catalunya, Barcelona, 08019, Spain
[5] IMCN Institute, Universite catholique de Louvain, Place Louis Pasteur 1, 1348 Louvain-la-Neuve, Belgium

E-mail: agata.przekora@umlub.pl

Abstract

The aim of this work was to evaluate the impact of atmospheric pressure nitrogen plasma on viability, proliferation, and osteogenic differentiation of normal mouse calvarial preosteoblasts (MC3T3-E1 Subclone 4), which were maintained in Hanks' balanced salt solution (HBSS) during plasma exposure. Obtained results clearly demonstrated that short-time (4, 8, and 16 s) nitrogen plasma treatment is non-toxic to the MC3T3-E1 cells, does not affect cell morphology, promotes preosteoblasts' proliferation, enhances osteogenic differentiation by increasing bone alkaline phosphatase and osteocalcin concentration, but inhibits mineralization of extracellular matrix. The best results were achieved for 16 s exposure time and when the preosteoblasts were left in HBSS for 3 h after plasma treatment. Presented studies indicate great clinical potential of cold atmospheric nitrogen plasma for regenerative medicine applications to improve bone healing process.

Keywords: plasma activated cells, GlidArc, plasma activated medium, cell viability, ECM mineralization

(Some figures may appear in colour only in the online journal)

J. Phys. D: Appl. Phys. **52** (2019) 275401

A Przekora *et al*

1. Introduction

Plasma technology synergistically utilizes impact of active species, high electric fields, and electromagnetic radiation to enhance efficiency and achieve targeted treatment goals [1]. When oxygen or nitrogen are used as substrate gas in ambient conditions, reactive oxygen and nitrogen species (RONS) are formed which can affect properties of inanimate materials and living organisms. Electrical discharge can occur directly in treated liquid or in the gas intrusions in the liquid phase. Moreover, plasma can interact with liquid indirectly when the discharge occurs in gaseous phase in the vicinity of the surface: the active species are then transferred via surface to the bulk of liquid. In the case of oxygen, this leads to formation of reactive radical species such as hydroxyl, hydrogen, superoxide, perhydroxyl and oxide anions, and molecular species such as hydrogen peroxide and ozone. Nitrogen-based species such as nitrogen oxide radicals, nitrate and nitrite anions, peroxynitrite, and also nitric, nitrous and peroxynitrous acids are also formed [1–7].

Atmospheric pressure plasma is utilized in various fields such as agriculture, food industry, engineering of biomaterials, exhaust gas, soil, water, and wastewater treatment [8–14]. For biotechnology and medical fields, plasma reactors working with targets in humid/wet environments are of high importance. Low temperature plasma for medical purposes was applied for inactivation of microorganisms in biofilm or planctonic forms and for decreasing of virulence [15–17]. There are reports on plasma-based bleeding control devices [18], plasma-supported cell boosting, plasma-induced wound healing, and application of plasma in regenerative medicine [19], where low temperature plasma can be utilized for increasing the material biocompatibility and enhancement of drug delivery [20, 21]. Many research teams work on elimination of cancer cells and enhancement of antitumor drug activity via low temperature plasma technology [22–25], some reports focus on gene therapy [26], mutagenicity [27] and state that application of low temperature plasma can promote differentiation of stem cells [28]. According to Tominami *et al*, short time application of plasma generated in a jet-type reactor can stimulate preosteoblasts' differentiation and accelerate periodontitis healing by promoting bone regeneration and bactericidal action [29].

The gliding arc discharge (GlidArc, GAD) belongs to the group of non-thermal plasmas, although it is formed from an electric arc discharge. The arc is generated between two diverging electrodes and it is blown along them by very fast transverse gas flow. The gas nozzle is placed between the electrodes in their axis of symmetry. The arc initiates at the shortest gap between the two electrodes and after it elongates by the fast gas flow from its initial position [12]. As the arc is elongated, its current is at its maximum and the voltage at the minimum. Arc elongation effects in increase in arc resistance, what implicates that elongating arc demands more and more power to be sustained, until it reaches the maximum that the power supply can provide and discharge extinguishes. After this transition point for the regime of GAD operation an initiation of the next cycle takes place. This is the transition point for the regime of GAD operation. The discharge is often effectively used for the process of disposal and treatment of different gaseous pollutants. Miscellaneous applications include bactericidal decontamination and treatment of seeds [12, 13].

The objective of this work was to identify the impact of atmospheric pressure plasma, generated in versatile GAD reactor working with nitrogen gas, on viability, proliferation, and osteogenic differentiation of normal mouse calvarial preosteoblasts (MC3T3-E1 Subclone 4). MC3T3-E1 cell line is a good model for studying osteogenic differentiation and bone formation under *in vitro* conditions since MC3T3-E1 cells exhibit similar behavior to primary calvarial osteoblasts [30].

2. Materials and methods

2.1. Plasma generator and performance

The compact experimental set up with mini GAD reactor that was used in this study is presented in figure 1. The mini GAD mini reactor is a small, light and portable reactor in a round casing with a diameter of 90 mm and a height of 130 mm. It was operated at the atmospheric pressure and consisted of two diverging profiled copper rod electrodes of 10 cm and 12° angle between them. The initial, smallest inter-electrode gap was settled as 3 mm and electrode tips were positioned at 3 cm distance from the surface of the sample. The flow-rate of nitrogen was 7.33 dm^3 min^{-1}. Electrical parameters were measured using a Tektronix P6015A voltage probe, Tektronix P6022 current probe and Tektronix TDS 2024B oscilloscope. Utilized GAD power supply was based on electronic high-voltage transformer of 50 Hz operation cycle. Maximum apparent power, calculated as the product of root mean square (RMS) values of current and voltage, was 52 VA and 25 VA on primary (U_1, I_1) and secondary side (U_2, I_2) of transformer, respectively. RMS voltage and current on the secondary side ranged 688 V and 36 mA, respectively. Voltage and current measurements were made using a Tektronix P6015A voltage probe, Tektronix P6022 current probe and Tektronix TDS 2024B oscilloscope. The figures 1(b) and (c) show a close-up on voltage and current waveforms. Their irregular shape of signals resulted not only from the characteristics of the generator, but above all from the random nature of the arc discharge. However, periodicity can be noticed, where higher voltage and current values corresponded to the duration of arcing, which appeared with the network frequency (50 Hz).

Since composition of gaseous phase may have a strong impact on RONS diffusion to the liquid phase [31], NO_2, NO, and CO concentrations were measured in the gas phase (one centimeter above the liquid) with the use of IBRID MX-6 sensor and concentration of ozone with the use of Ozone ECO-Sensors A-21ZX. Sensors' sensitivity was as follows: 1 ppm for CO, 0.01 ppm for ozone, 0.1 ppm for NO and NO_2. The gas was pumped through a 30 cm tube and supplied to the sensors through device adapters (figure 1(a)). During the measurements, no additional ventilation was used. GAD plasma source—which is known for efficient generation of NO_x— allowed for relatively high formation of NO
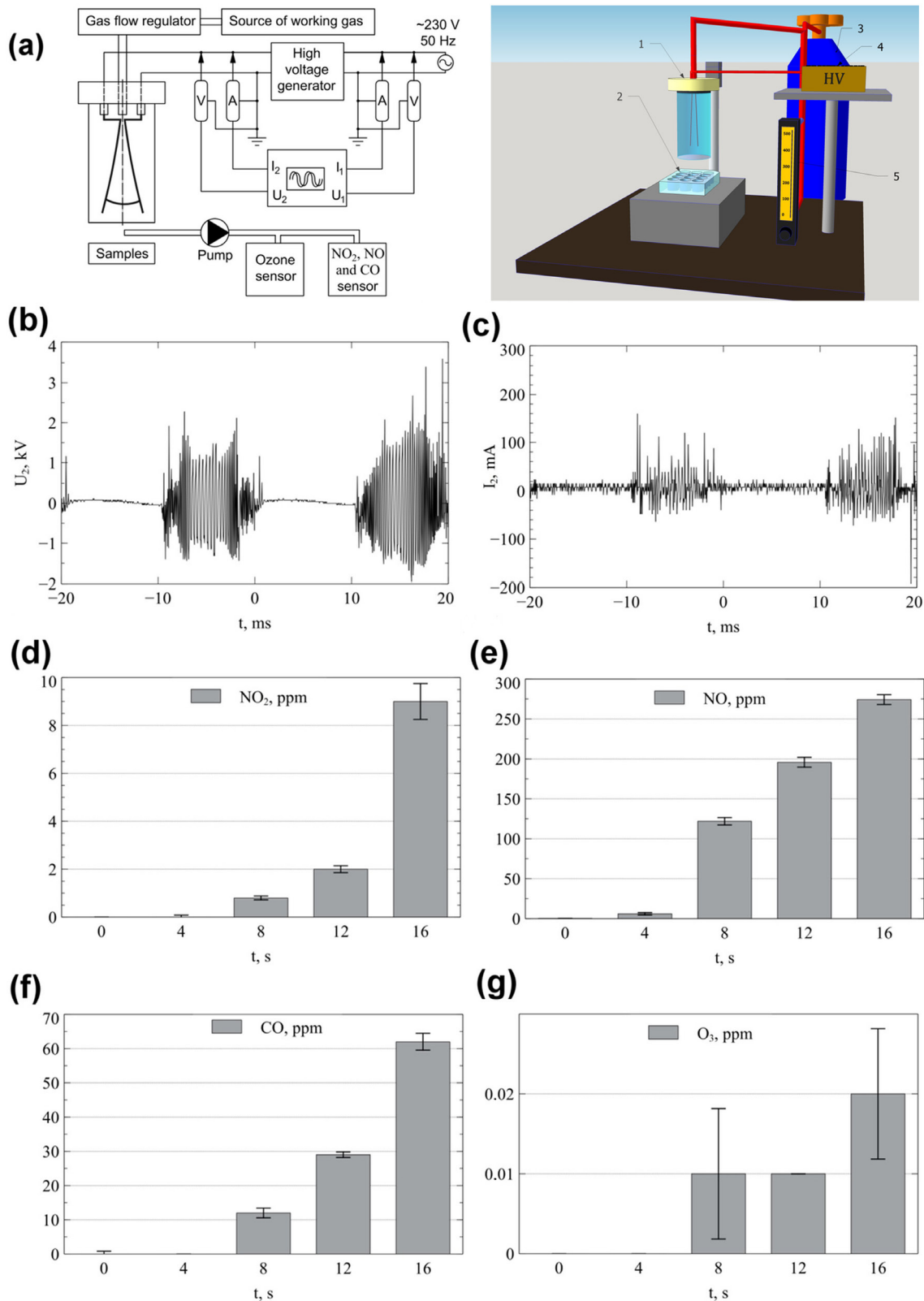
Figure 1. (a) Schematic diagrams of the experimental setup: 1—GAD reactor, 2—96-multiwell plate with MC3T3-E1 cells, 3—gas supply, 4—electric power source, 5—flowmeter; (b) typical voltage of mini-GAD; (c) typical current characteristics of mini-GAD; (d)–(g)—concentration of NO_2, NO, CO, and O_3 in a gaseous phase, respectively.

J. Phys. D: Appl. Phys. **52** (2019) 275401

A Przekora *et al*

reaching 274 ppm in a short 16 s time, whereas concentration of other gas components were relatively low ($NO_2 - 9$ ppm, $CO - 62$ ppm, $O_3 - 0.02$ ppm) but increased with the treatment time. Figures 1(d)–(g) show the results averaged from three measurements with the standard deviation as a measurement error.

2.1.1. Plasma treatment of the cells. Adherent MC3T3-E1 preosteoblasts cultured in polystyrene wells of 96-multiwell plate were exposed to plasma for 4 s, 8 s, and 16 s. Before GAD treatment with the use of nitrogen as a substrate gas, growth medium was discarded and replaced with 100 μl of Hanks' balanced salt solution (HBSS, Sigma-Aldrich Chemicals) to provide uniform environment during plasma exposure and to avoid unexpected results due to the high complexity of the composition of growth medium [32]. Temperature of the surface of the HBSS in a well with MC3T3-E1 cells was measured just after plasma exposure with uninsulated K-type thermocouple with electronic temperature compensation multimeter and did not exceed 23 °C. Evaporation process caused by the gas flow and slightly elevated gas temperature was not observable during short 16 s treatment time.

2.2. Cell culture

The experiments were carried out using mouse calvarial preosteoblast cell line (MC3T3-E1 Subclone 4) purchased from ATCC (American Type Culture Collection). MC3T3-E1 preosteoblasts were cultured in Minimum Essential Medium Eagle—Alpha Modification (alpha MEM medium, GIBCO) supplemented with 10% fetal bovine serum (Pan-Biotech) and antibiotics (100 U ml^{-1} penicillin, 100 μg ml^{-1} streptomycin) supplied by Sigma-Aldrich Chemicals. The cells were maintained in an incubator at 37 °C in a humidified atmosphere of 5% CO_2 and 95% air.

2.2.1. Evaluation of cell viability after GAD treatment. To assess the effect of plasma treatment on preosteoblasts' viability, MC3T3-E1 cells were seeded in 100 μl of the complete growth medium in 96-multiwell plates at a concentration of 3×10^4 cells/well and cultured for 24 h at 37 °C. Before GAD treatment, growth medium was discarded and replaced with 100 μl of HBSS. Preosteoblasts were exposed to plasma for 4 s, 8 s, and 16 s. Immediately ($t = 0$) as well as 3 h ($t = 3$ h) after GAD treatment, HBSS was discarded and fresh growth medium was added to each well. The cells were cultured for further 24 h and cell viability was assessed using 3-(4,5-dimethylthiazol-2-yl)-2,5-diphenyltetrazolium bromide-based assay known as MTT (Sigma-Aldrich Chemicals). Briefly, 25 μl of MTT solution (5 mg ml^{-1} in phosphate buffered saline—PBS, Sigma-Aldrich Chemicals) were added to each well and the cells were returned to the CO_2 incubator for 3 h. Then, formazan crystals produced by viable cells were dissolved using 100 μl of 10% sodium dodecyl sulfate (SDS)-HCl solution (Sigma-Aldrich Chemicals). After 12 h of incubation, the absorbance was measured at 570 nm using BioTek Synergy H4 Hybrid Microplate Reader. Viability of cells was expressed as the percentage of absorbance values obtained with respect to the control untreated cells (showing 100% viability), which were maintained in HBSS in an analogous manner to plasma-treated cells ($t = 0$ and $t = 3$ h).

2.2.2. Evaluation of cell proliferation after GAD treatment. MC3T3-E1 cells were seeded in 100 μl of the complete culture medium in 96-multiwell plates at very low concentration of 3×10^3 cells/well and cultured for 24 h at 37 °C. Before GAD treatment, growth medium was discarded and replaced with 100 μl of HBSS. Preosteoblasts were exposed to plasma for 4 s, 8 s, and 16 s. Immediately ($t = 0$) as well as 3 h ($t = 3$ h) after plasma exposure, HBSS was replaced with fresh growth medium and the cells were cultured for further 3 d. On the 1st, 2nd, and 3rd day of the experiment, cell proliferation was assessed colorimetrically using Cell Counting Kit-8 which is based on water-soluble tetrazolium salt (WST-8, Sigma-Aldrich Chemicals). Exact cell number was quantified from a calibration curve prepared for known concentrations of preosteoblasts. The test was performed according to the manufacturer's protocol. Untreated cells (that were not exposed to plasma) served as a control. Viable cell numbers as determined by WST-8 test for each time interval were then entered in Doubling Time Computing software to calculate the growth rate and doubling time.

2.2.3. Evaluation of cell morphology after GAD treatment. Since WST-8 is non-toxic to the cells, after proliferation testing (on the 3rd day), the MC3T3-E1 preosteoblasts were washed with PBS and stained with AlexaFluor635phalloidin (Life Technologies, Thermo Fisher Scientific) and 4′,6-diamidino-2-phenylindol (DAPI, Sigma-Aldrich Chemicals). Before fluorescent staining, the cells were fixed with 3.7% formaldehyde solution (Sigma-Aldrich Chemicals) for 10 min at room temperature and permeabilized with 0.2% TritonX-100 (Sigma-Aldrich Chemicals) for 15 min. Cell cytoskeleton and nuclei were stained for 20 min at room temperature using two units of phallotoxin and 0.5 μg ml^{-1} DAPI. Morphology of stained cells was analyzed under a fluorescence laser scanning microscope, using a 2D scan technique (Olympus Fluoview equipped with an FV1000 laser scanner).

2.2.4. Evaluation of osteogenic differentiation after GAD treatment. MC3T3-E1 cells were seeded in 96-multiwell plates and treated with GAD in the same manner as in the case of viability assessment (section 2.2.1). Immediately ($t = 0$) as well as 3 h ($t = 3$ h) after plasma exposure, HBSS was replaced with freshly prepared osteogenic medium containing 0.05 mg ml^{-1} ascorbic acid and 10 mM β-glycerophosphate (Sigma-Aldrich Chemicals). The cells were cultured for further 13 or 21 d and then osteogenic differentiation was determined by evaluation of bone alkaline phosphatase (BAP) and osteocalcin (OC) concentration by enzyme-linked immunosorbent assays—ELISAs (muALPL ELISA kit, Uscn Life Science Inc. and muOC ELISA kit, Immunotopics Inc., respectively), which were performed according to the manufacturers' protocols. Briefly, standards (BAP or OC) and samples were added

J. Phys. D: Appl. Phys. **52** (2019) 275401

A Przekora *et al*

Table 1. Doubling time (in hours) and growth rate (number of doublings per hour) calculated for MC3T3-E1 cells after exposure to GAD.

Proliferation parameters	$t = 0$				$t = 3$ h			
	Control	4 s	8 s	16 s	Control	4 s	8 s	16 s
Doubling time	38	41	33	33	39	32	31	32
Growth rate	0.0182	0.0169	0.0210	0.0209	0.0175	0.0215	0.0221	0.0213

to the appropriate wells of ELISA microplates, which were pre-coated by manufacturers with the antibodies specific to BAP or OC (sandwich ELISA). Then, biotin-conjugated polyclonal antibodies specific to BAP or OC were added followed by the addition of Avidin conjugated to horseradish peroxidase (HRP) in the case of muALPL ELISA or secondary antibodies conjugated to HRP in the case of muOC ELISA. The 3,3′,5,5′-tetramethylbenzidine (TMB) was used a substrate for HRP. The enzyme-substrate reaction was terminated by the addition of a sulfuric acid solution and the absorbance was spectrophotometrically measured at a wavelength of 450 nm. BAP concentration (early differentiation marker) was determined on the 13th day of the experiment in the cell lysates prepared according to the procedure described earlier [29]. Concentration of intact OC (late differentiation marker) was determined on the 13th and 21st day in the cell culture supernatants.

MC3T3-E1 mineralization (the last stage of osteogenic differentiation) was assessed on the 21st day by determination of deposition of calcium phosphates in the extracellular matrix (ECM). Briefly, preosteoblasts were gently washed with HBSS without calcium and magnesium and the cells were decalcified by addition of 40 μl of 0.5 M HCl (Avantor Performance Materials Poland). Afterwards, the plates were sealed with parafilm to avoid evaporation and stored at 4 °C for at least 24 h (or until use). Calcium and phosphate concentrations in the samples were determined by colorimetric methods using commercially available Ca^{2+} and HPO_4^{2-} detection kits (BioMaxima Poland).

2.3. Statistical analysis

All tests were repeated in at least two experiments which were performed in quadruplicate. The statistically significant results (considered at a probability of $P < 0.05$) compared to the control untreated cells were determined using an unpaired *t*-test (GraphPad Prism 5, Version 5.03 Software).

3. Results

3.1. Cell viability

GAD treatment only slightly decreased cell viability regardless of the time of exposure (figure 2). Viability of cells was high (above 80%) which is considered as the threshold for cytotoxicity of tested compounds/stimulations, and thus indicating the non-toxicity of nitrogen plasma against these
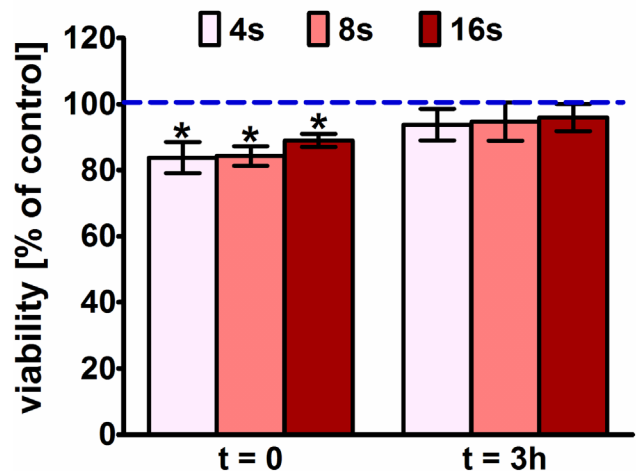

Figure 2. Viability of MC3T3-E1 preosteoblasts upon exposure to GAD assessed by MTT assay ($t = 0$—HBSS replaced with growth medium immediately after GAD treatment, $t = 3$ h—HBSS replaced with growth medium 3 h after GAD treatment); *significantly different results compared to the untreated control cells according to unpaired *t*-test, $P < 0.05$.

preosteoblastic cells. Interestingly, MC3T3-E1 cells left in HBSS for 3 h after GAD treatment showed higher viability (approx. 95%) than cells where HBSS was immediately replaced by cell culture medium (approx. 85%).

3.2. Cell proliferation

MC3T3-E1 cells exposed to GAD treatment revealed faster growth rate and shorter doubling time (in the range of 31–33 h) compared to the control untreated cells (38–39 h) (table 1). In the case of cells that had HBSS immediately changed after GAD treatment ($t = 0$), enhanced proliferation was observed only after longer plasma exposure times (8 s and 16 s). Moreover, when the longer GAD treatment was applied, faster proliferation was observed (figure 3(a)). On the 3rd day there were $17.13 \pm 1.21 \times 10^3$ control untreated cells, whereas after plasma exposure there were $19.89 \pm 1.50 \times 10^3$ cells for 8 s treatment and $22.19 \pm 2.13 \times 10^3$ cells for 16 s GAD treatment. However, in the case of cells left in HBSS for 3 h after plasma treatment, RONS formed in HBSS promoted preosteoblasts' proliferation regardless of plasma exposure time (figure 3(b)). On the 3rd day there were approx. $22–23 \times 10^3$ cells for 4, 8, and 16 s GAD treatment, which was significantly more compared to the control untreated cells ($16.62 \pm 1.00 \times 10^3$ cells).
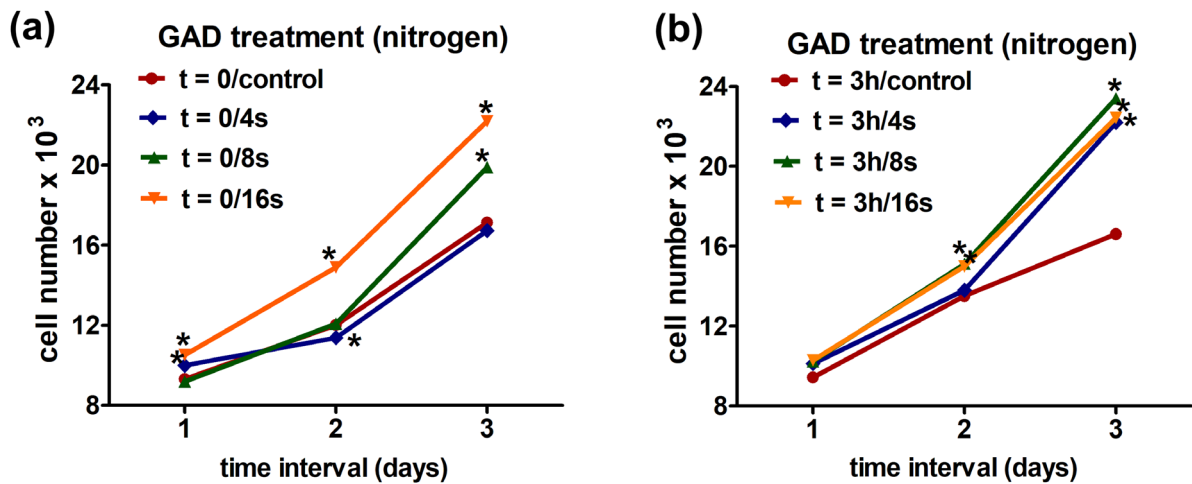
Figure 3. Proliferation of MC3T3-E1 preosteoblasts upon exposure to GAD assessed by WST-8 assay: (a) HBSS replaced with growth medium immediately after GAD treatment, (b) HBSS replaced with growth medium 3 h after GAD treatment; *significantly different results compared to the untreated control cells according to unpaired *t*-test, $P < 0.05$.
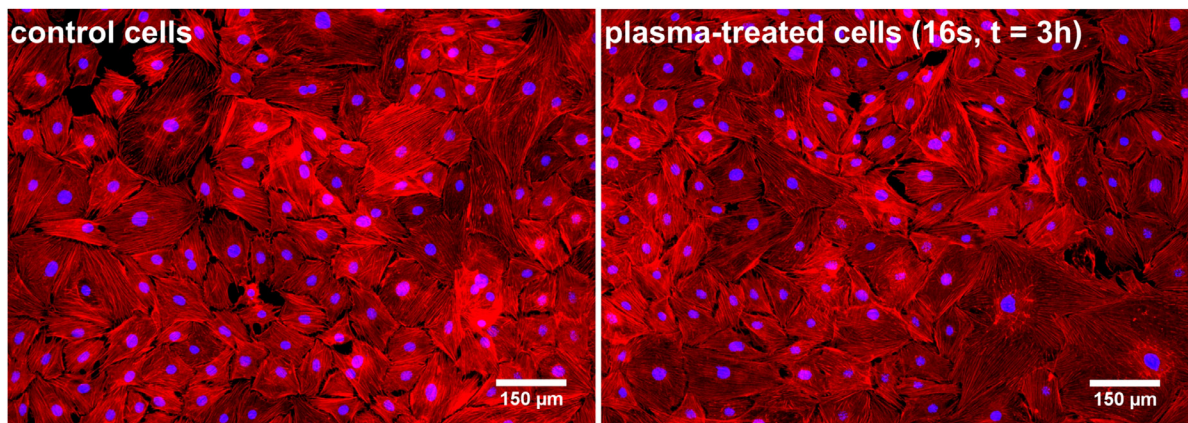

Figure 4. Images presenting morphology of control untreated preosteoblasts and MC3T3-E1 cells after 16 s GAD treatment and HBSS replaced with growth medium 3 h after plasma exposure (red fluorescence—F-actin filaments of cell cytoskeleton, blue fluorescence—cell nuclei).

3.3. Cell morphology

Microscopy observation of cells revealed that plasma treatment did not affect morphology of MC3T3-E1 preosteoblasts regardless of plasma exposure time and incubation period in HBSS ($t = 0$ or $t = 3$ h). Sample images are presented in figure 4. Both untreated and plasma-exposed cells were well spread and had extensive cytoskeleton structure. Importantly, nitrogen plasma did not exert any negative effect on MC3T3-E1 morphology.

3.4. Osteogenic differentiation

On the 13th day of the experiment it was observed that nitrogen plasma slightly (but statistically significantly) increased BAP and OC concentration only in the case of MC3T3-E1 cells exposed to plasma for 16 s and left in HBSS for 3 h after GAD treatment (figures 5 and 6(a)). Concentration of BAP and OC in untreated control cultures was equal to 3.67 ± 0.09 ng ml^{-1} and 10.37 ± 0.38 ng ml^{-1}, respectively, whereas concentration of BAP and OC in GAD-treated cultures (16 s, $t = 3$ h) was equal to 4.68 ± 0.21 ng ml^{-1} and 13.37 ± 0.73 ng ml^{-1},
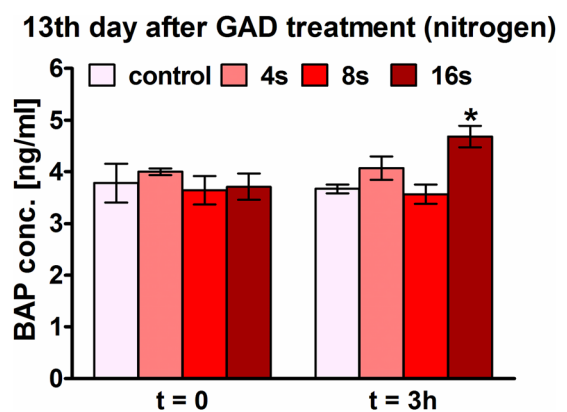

Figure 5. BAP concentration in MC3T3-E1 cultures upon exposure to GAD assessed by ELISA; *significantly different results compared to the untreated control cells according to unpaired *t*-test, $P < 0.05$.

respectively. On the 21st day of the experiment, OC synthesis was significantly enhanced compared to the control cells (approx. 13 ng ml^{-1}) in all GAD-treated MC3T3-E1 cells with HBSS exchanged after 3 h (approx. 16–17 ng ml^{-1})
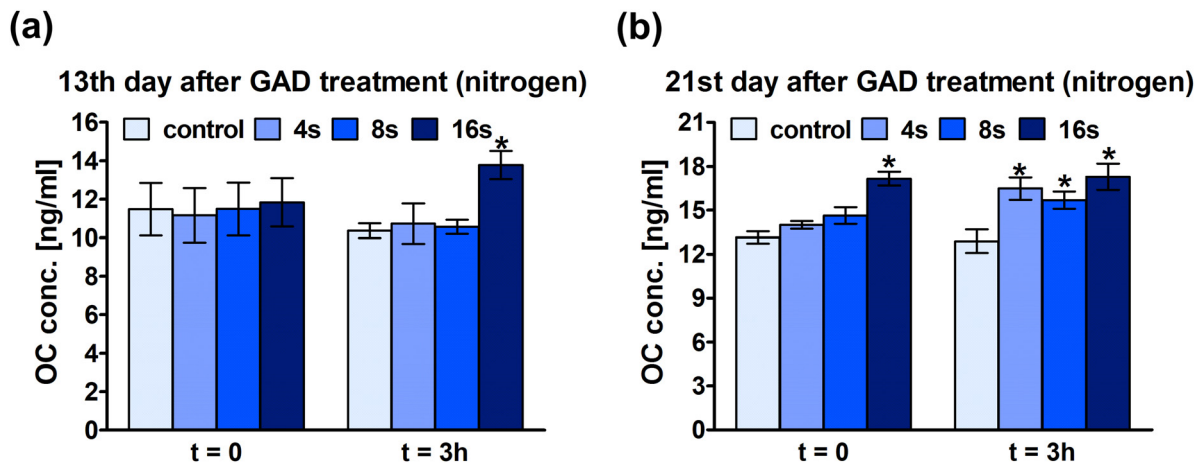
Figure 6. OC production by MC3T3-E1 preosteoblasts assessed by ELISA: (a) OC concentration determined 13 d after exposure to GAD, (b) OC concentration determined 21 d after exposure to GAD; *significantly different results compared to the untreated control cells according to unpaired *t*-test, $P < 0.05$.
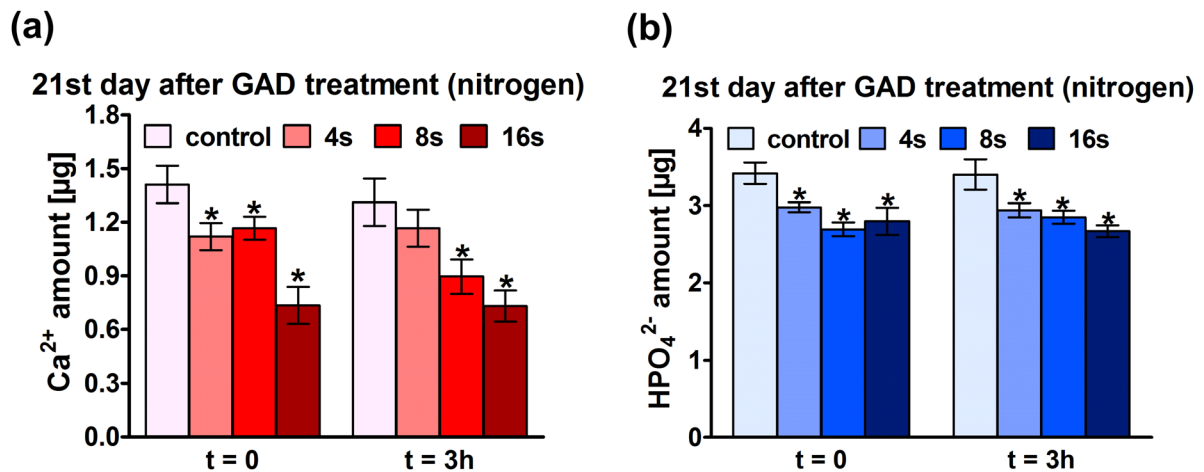

Figure 7. Mineralization of MC3T3-E1 osteoblasts upon exposure to GAD assessed by colorimetric methods via determination of Ca^{2+} and HPO_4^{2-} amounts in the cultures: (a) Ca^{2+} amounts in MC3T3-E1 cultures, (b) HPO_4^{2-} amounts in MC3T3-E1 cultures; *significantly different results compared to the untreated control cells according to unpaired *t*-test, $P < 0.05$.

and in preosteoblasts treated with plasma for 16 s with HBSS exchanged immediately after exposure (approx. 17 ng ml^{-1}) (figure 6(b)).

RONS formed after GAD treatment negatively affected ECM mineralization in preosteoblasts even after short 4 s plasma exposure time. MC3T3-E1 cells treated with plasma for 16 s (both $t = 0$ and $t = 3$ h) revealed almost 2-fold lower Ca^{2+} amount (approx. 0.7 μg) compared to the untreated cells (approx. 1.4 μg) (figure 7(a)). Phosphate amount detected in GAD-treated cultures (approx. 2.7-2.9 μg) was reduced by approx. 15%–20% compared to untreated control preosteoblasts (approx. 3.4 μg) (figure 7(b)). Moreover, the longer the GAD treatment was applied, the lower the amounts of calcium and phosphate ions were determined, which was clearly observed in the case of cultures left for 3 h in HBSS after plasma exposure.

4. Discussion

Hydroxyl radicals, hydrogen peroxide (H_2O_2), and superoxide belong to reactive oxygen species (ROS) which may be produced under various physiological (e.g. natural process of aging) as well as pathological conditions (e.g. cerebellar ischemia, atherosclerosis, sunburns). Excessive ROS generation may induce oxidative stress causing cell injury and death. Nevertheless, some reports identified also the crucial role of ROS in the regulation of cell metabolism, proliferation, and differentiation [33].

Plasma is known to have ability to generate different reactive species showing a variety of biological activities, like promotion of wound healing process or prevention against microbial infections. Importantly, these biological actions of plasma were primarily observed in liquid environment

J. Phys. D: Appl. Phys. **52** (2019) 275401

A Przekora *et al*

indicating that reactive species produced by plasma in the gas phase can be transferred through diffusion and secondary reactions to a liquid, to produce singlet oxygen ($^1O_2$), hydroxyl radicals (OH), nitric oxide radicals (NO), hydrogen peroxide (H_2O_2), etc [34]. Moreover, it is known that plasma generates different RONS in liquids depending on the substrate gas used. Takamatsu *et al* used in their experiment the multi-gas plasma jet which generated (at low gas temperatures) atmospheric plasma of oxygen, argon, nitrogen, carbon dioxide, helium, and air. They measured and compared concentrations of various reactive species ($^1O_2$, OH radicals, H radicals, and NO radicals) formed by different plasmas in a solution (phosphate buffered saline, PBS). The results demonstrated that nitrogen plasma produced the largest amount of OH radicals (which may further react to form H_2O_2) among all tested homo-atomic gas species. Moreover, nitrogen plasma was also proved to generate large amounts of H and NO radicals [34]. Different works have shown that a variety of RONS are formed in liquids depending on their composition and the plasma parameters, and usually higher amounts of RONS are formed in cell culture media due to the rich content in biomolecules [35].

In this research, it was shown that the interaction of nitrogen plasma with HBSS and the cells significantly enhanced proliferation of MC3T3-E1 preosteoblasts (table 1, figure 3). In other works different mechanisms have been pointed out. Kalghatgi *et al* demonstrated that 30 s exposure of endothelial cells to non-thermal dielectric barrier discharge (DBD) air plasma significantly enhanced their proliferation due to ROS-mediated fibroblast growth factor-2 (FGF-2) release. They implied that FGF-2 release upon plasma treatment was most likely related to generation of neutral ROS, like O_3, NO, H_2O_2, or OH [36]. It should be noted that FGF-2 is also produced by osteoblastic cells and is known to regulate osteoblast functions by acting as an autocrine or paracrine signal for bone cells [37, 38]. Moreover, Dupree *et al* proved that FGF-2 possesses the ability to enhance proliferation potential of osteoblasts and bone marrow-derived mesenchymal stem cells [39]. Thus, it may be assumed that the observed enhanced preosteoblasts' proliferation probably resulted here also from RONS-mediated FGF-2 release. Nevertheless, Tominami *et al* showed that although cold atmospheric helium plasma generated large amount of H_2O_2, OH, and superoxide anion radicals, they did not have any positive effect on proliferation of MC3T3-E1 preosteoblasts [29].

Other available in the literature works employing plasma jet exposure of osteoblast-like cells (osteosarcoma-derived cells) were related to apoptotic death of tumor cells. In that case longer treatment times were used than here, which clearly indicates the importance of plasma dosing to either induce cytotoxicity [32, 40, 41] or enhance cell proliferation, as in our work. Even shorter treatment times with other kinds of sources, such as the well-established kINPen may lead to apoptotic cell death (only 10 s treatment led to compromised viability of human peripheral blood mononuclear cell, and impaired proliferation of immune system T-cells) [42]. This clearly underlines the importance of the configuration and

characteristics of the plasma source in the biological effects obtained.

The group of Freeman investigated chondrogenic and osteogenic differentiation in different works. They showed that exposure of mesenchymal stem cells to short (10 s) microsecond pulsed DBD increased ROS and ROS-associated signaling, enhancing both chondrogenic and osteogenic differentiation [43]. Mechanisms were further investigated by treatment of CH3/10T1/2 mouse embryonic cells cultured on type I collagen which showed increased expression of adhesion proteins (pFAK, FAK, Akt, Bcl-2) and activation of survival pathways (but very dependent on the plasma treatment conditions). In line with our findings, their results indicate plasma-induced and RONS-mediated chondrogenic differentiation and bone formation [44].

Similarly, in the present study, it was also demonstrated that nitrogen plasma treatment of preosteoblasts increased BAP (only for 16 s, $t = 3$ h) and OC concentration (figures 5 and 6) but inhibited cell mineralization (figure 7) in an irradiation-time-dependent manner. BAP is an early marker of bone formation process and its highest concentration is observed during the second phase of osteogenic differentiation (ECM synthesis stage). Unlike BAP, OC is the marker of the late stage of osteogenic differentiation associated with ECM mineralization since OC is a mineral binding protein. Nevertheless, OC is also produced by osteoblasts during the second stage of differentiation [45–47]. Interestingly, despite increased OC concentration detected in plasma-treated cultures, ECM mineralization was significantly reduced. Arai *et al* demonstrated that MC3T3-E1 cells exposed to non-toxic concentrations of H_2O_2 revealed significantly increased expression of genes for OC and at the same time 2-fold lower mineralization level compared to the untreated cells. They assumed that H_2O_2 caused up-regulation of antioxidant system altering osteogenic gene expression [33]. Therefore, it may be suggested that nitrogen plasma treatment of MC3T3-E1 cells caused RONS-related change in the expression of osteogenic genes, promoting mainly the second stage of the differentiation process—ECM synthesis, and inhibiting the last stage—ECM mineralization. However, contrary results were obtained by Tominami *et al* who demonstrated that cold atmospheric helium plasma treatment (generating H_2O_2, OH, and superoxide anion radicals) of MC3T3-E1 preosteoblasts' resulted in enhanced mineralization and increased BAP activity [29]. Nevertheless, it should be noted that application of helium gas undoubtedly resulted in the formation of different RONS (at different concentrations) from that formed after nitrogen plasma.

The effect of reactive species generated by various plasmas on living cells may be very complex at the molecular level. Moreover, it is known that the nature and concentration of reactive species formed after plasma exposure may vary a lot depending on the substrate gas used for the experiments, experimental setup (type of plasma reactor), the distance (height) between the electrodes and the liquid, or the type of plasma activated liquid. All this parameters which modify plasma-induced RONS, but also the electromagnetic fields and

J. Phys. D: Appl. Phys. **52** (2019) 275401

A Przekora *et al*

UV–vis radiation in contact with the biological system have an impact on cell proliferation and differentiation *in vitro*. No exact plasma system as the one presented here with nitrogen has been employed, although some of the mechanisms discussed may be extrapolated to the modulation of osteoblast behavior, and be used to further investigate in this line.

5. Conclusion

Presented results clearly demonstrated that short-time nitrogen plasma treatment is non-toxic to the MC3T3-E1 cells, does not affect cell morphology, promotes proliferation of preosteoblasts, enhances osteogenic differentiation by increasing BAP and OC concentration, but inhibits ECM mineralization process. During plasma treatment, oxygen and nitrogen radicals are formed, which have great impact on cell behavior. Thus, the best results were achieved for 16 s exposure time and when the preosteoblasts were left in HBSS for 3 h after plasma treatment. Based on the results obtained it may be inferred that short-time cold atmospheric nitrogen plasma treatment appears to have great clinical potential to be used in regenerative medicine applications for improvement of bone healing process by promotion of preosteoblasts' proliferation and bone ECM synthesis.

Acknowledgments

ORCID iDs

Agata Przekora https://orcid.org/0000-0002-6076-1309
Sophie Hermans https://orcid.org/0000-0003-4715-7964

References

[1] Pawłat J 2013 *Electrical Discharges in Humid Environments. Generators, Effects, Application* (Lublin: Politechnika Lubelska)

[2] Bruggeman P J *et al* 2016 Plasma-liquid interactions: a review and roadmap *Plasma Sources Sci. Technol.* **25** 053002

[3] Brisset J-L and Pawlat J 2016 Chemical effects of air plasma species on aqueous solutes in direct and delayed exposure modes: discharge, post-discharge and plasma activated water *Plasma Chem. Plasma Process.* **36** 355–81

[4] Lukes P, Dolezalova E, Sisrova I and Clupek M 2014 Aqueous-phase chemistry and bactericidal effects from an air discharge plasma in contact with water: evidence for the formation of peroxynitrite through a pseudo-second-order post-discharge reaction of H_2O_2 and HNO_2 *Plasma Sources Sci. Technol.* **23** 015019

[5] Machala Z, Tarabova B, Hensel K, Spetlikova E, Sikurova L and Lukes P 2013 Formation of ROS and RNS in water electro-sprayed through transient spark discharge in air and their bactericidal effects *Plasma Process. Polym.* **10** 649–59

[6] Girard F, Badets V, Blanc S, Gazeli K, Marlin L, Authier L, Svarnas P, Sojic N, Clément F and Arbault S 2016 Formation of reactive nitrogen species including peroxynitrite in physiological buffer exposed to cold atmospheric plasma *RSC Adv.* **6** 78457–67

[7] Girard F *et al* 2018 Correlations between gaseous and liquid phase chemistries induced by cold atmospheric plasmas in a physiological buffer *Phys. Chem. Chem. Phys.* **20** 9198–210

[8] Kučerová K, Henselová M, Slováková Ľ and Hensel K 2018 Effects of plasma activated water on wheat: Germination, growth parameters, photosynthetic pigments, soluble protein content, and antioxidant enzymes activity *Plasma Process. Polym.* **16** e1800131

[9] Kalra C S, Gutsol A F and Fridman A A 2005 Gliding arc discharges as a source of intermediate plasma for methane partial oxidation *IEEE Trans. Plasma Sci.* **33** 32–41

[10] Burlica R, Kirkpatrick M J and Locke B R 2006 Formation of reactive species in gliding arc discharges with liquid water *J. Electrost.* **64** 35–43

[11] Stará Z, Krčma F, Nejezchleb M and Dušan Skalný J 2009 Organic dye decomposition by DC diaphragm discharge in water: effect of solution properties on dye removal *Desalination* **239** 283–94

[12] Dasan B G, Onal-Ulusoy B, Pawlat J, Diatczyk J, Sen Y and Mutlu M 2017 A new and simple approach for decontamination of food contact surfaces with gliding arc discharge atmospheric non-thermal plasma *Food Bioprocess Technol.* **10** 650–61

[13] Pawlat J, Starek A, Sujak A, Kwiatkowski M, Terebun P and Budzeń M 2018 Effects of atmospheric pressure plasma generated in GlidArc reactor on Lavatera thuringiaca L. seeds' germination *Plasma Process. Polym.* **15** 1700064

[14] Pawlat J, Starek A, Sujak A, Terebun P, Kwiatkowski M, Budzeń M and Andrejko D 2018 Effects of atmospheric pressure plasma jet operating with DBD on Lavatera thuringiaca L. seeds' germination *PLoS One* **13** e0194349

[15] Ziuzina D, Boehm D, Patil S, Cullen P J and Bourke P 2015 Cold plasma inactivation of bacterial biofilms and reduction of quorum sensing regulated virulence factors *PLoS One* **10** e0138209

[16] Kovalová Z, Tarabová K, Hensel K and MacHala Z 2013 Decontamination of Streptococci biofilms and *Bacillus cereus* spores on plastic surfaces with DC and pulsed corona discharges *EPJ Appl. Phys.* **61** 24306

[17] Aboubakr H A, Mor S K, Higgins L, Armien A, Youssef M M, Bruggeman P J and Goyal S M 2018 Cold argon–oxygen plasma species oxidize and disintegrate capsid protein of feline calicivirus *PLoS One* **13** e0194618

[18] Masi G D *et al* 2018 Plasma coagulation controller: a low-power atmospheric plasma source for accelerated blood coagulation *Plasma Med.* **8** 245–54

[19] Arndt S *et al* 2013 Cold atmospheric plasma (CAP) changes gene expression of key molecules of the wound healing

machinery and improves wound healing *in vitro* and *in vivo* *PLoS One* **8** e79325

[20] Ponte G D, Sardella E, Fanelli F, d'Agostino R and Favia P 2011 Trends in surface engineering of biomaterials: atmospheric pressure plasma deposition of coatings for biomedical applications *Eur. Phys. J. Appl. Phys.* **56** 24023

[21] Canal C, Modic M, Cvelbar U and Ginebra M-P 2016 Regulating the antibiotic drug release from β-tricalcium phosphate ceramics by atmospheric plasma surface engineering *Biomater. Sci.* **4** 1454–61

[22] Mine K, Miyamaru Y, Hayashi N, Aijima R and Yamashita Y 2017 Mechanism of inactivation of oral cancer cells irradiated by active oxygen species from DBD plasma *Plasma Med.* **7** 201–13

[23] Metelmann P H, Nedrelow D S, Schuster M, Rutkowski R and Seebauer C 2016 Clinical studies applying physical plasma in head and neck cancer—key points and study design *Int. J. Clin. Res. Trials* **1** 103

[24] Recek N, Cheng X, Keidar M, Cvelbar U, Vesel A, Mozetic M and Sherman J 2015 Effect of cold plasma on glial cell morphology studied by atomic force microscopy *PLoS One* **10** e0119111

[25] Park S-B, Kim B, Bae H, Lee H, Lee S, Choi E H and Kim S J 2015 Differential epigenetic effects of atmospheric cold plasma on MCF-7 and MDA-MB-231 breast cancer cells *PLoS One* **10** e0129931

[26] Isozaki Y, Ikeda Y, Kido Y, Satoh S and Jinno M 2017 Reactive oxygen species and intracellular Ca^{2+} contribution to micro-discharge plasma gene transfection *Plasma Med.* **7** 321–32

[27] Kim K C *et al* 2017 Exposure of keratinocytes to non-thermal dielectric barrier discharge plasma increases the level of 8—oxoguanine via inhibition of its repair enzyme *Mol. Med. Rep.* **16** 6870–5

[28] Nishihara S, Ota H and Miura T 2017 Atmospheric pressure plasma irradiation on embryonic stem cells: signals and differentiation *Plasma Med.* **7** 215–25

[29] Tominami K, Kanetaka H, Sasaki S, Mokudai T, Kaneko T and Niwano Y 2017 Cold atmospheric plasma enhances osteoblast differentiation *PLoS One* **12** e0180507

[30] Przekora A 2019 The summary of the most important cell-biomaterial interactions that need to be considered during *in vitro* biocompatibility testing of bone scaffolds for tissue engineering applications *Mater. Sci. Eng.* C **97** 1036–51

[31] Schmidt-Bleker A, Winter J, Bösel A, Reuter S and Weltmann K-D 2016 On the plasma chemistry of a cold atmospheric argon plasma jet with shielding gas device *Plasma Sources Sci. Technol.* **25** 015005

[32] Canal C, Fontelo R, Hamouda I, Guillem-Marti J, Cvelbar U and Ginebra M-P 2017 Plasma-induced selectivity in bone cancer cells death *Free Rad. Biol. Med.* **110** 72–80

[33] Arai M, Shibata Y, Pugdee K, Abiko Y and Ogata Y 2007 Effects of reactive oxygen species (ROS) on antioxidant system and osteoblastic differentiation in MC3T3-E1 cells *IUBMB Life* **59** 27–33

[34] Takamatsu T, Uehara K, Sasaki Y, Miyahara H, Matsumura Y, Iwasawa A, Ito N, Azuma T, Kohno M and Okino A 2014 Investigation of reactive species using various gas plasmas *RSC Adv.* **4** 39901–5

[35] Khlyustova A, Labay C, Ginebra M-P and Canal C 2019 Production of RONS in liquids by plasma jets for plasma medicine *Frontiers Chem. Sci. Eng.* (https://doi.org/10.1007/s11705-019-1801-8)

[36] Kalghatgi S, Friedman G, Fridman A and Clyne A M 2010 Endothelial cell proliferation is enhanced by low dose non-thermal plasma through fibroblast growth factor-2 release *Ann. Biomed. Eng.* **38** 748–57

[37] Shimoaka T, Ogasawara T, Yonamine A, Chikazu D, Kawano H, Nakamura K, Itoh N and Kawaguchi H 2002 Regulation of osteoblast, chondrocyte, and osteoclast functions by fibroblast growth factor (FGF)-18 in comparison with FGF-2 and FGF-10 *J. Biol. Chem.* **277** 7493–500

[38] Chikazu D, Katagiri M, Ogasawara T, Ogata N, Shimoaka T, Takato T, Nakamura K and Kawaguchi H 2001 Regulation of osteoclast differentiation by fibroblast growth factor 2: stimulation of receptor activator of nuclear factor κB ligand/osteoclast differentiation factor expression in osteoblasts and inhibition of macrophage colony-stimulating factor function in osteoclast precursors *J. Bone Miner. Res.* **16** 2074–81

[39] Dupree M A, Pollack S R, Levine E M and Laurencin C T 2006 Fibroblast growth factor 2 induced proliferation in osteoblasts and bone marrow stromal cells: a whole cell model *Biophys. J.* **91** 3097–112

[40] Gümbel D, Bekeschus S, Gelbrich N, Napp M, Ekkernkamp A, Kramer A and Stope M B 2017 Cold atmospheric plasma in the treatment of osteosarcoma *Int. J. Mol. Sci.* **18** 2004

[41] Gümbel D, Suchy B, Wien L, Gelbrich N, Napp M, Kramer A, Ekkernkamp A, Daeschlein G and Stope M B 2017 Comparison of cold atmospheric plasma devices' efficacy on osteosarcoma and fibroblastic *in vitro* cell models *Anticancer Res.* **37** 5407–14

[42] Bekeschus S, Masur K, Kolata J, Wende K, Schmidt A, Bundscherer L, Barton A, Kramer A, Bröker B and Weltmann K-D 2013 Human mononuclear cell survival and proliferation is modulated by cold atmospheric plasma jet *Plasma Process. Polym.* **10** 706–13

[43] Steinbeck M J, Chernets N, Zhang J, Kurpad D S, Fridman G, Fridman A and Freeman T A 2013 Skeletal cell differentiation is enhanced by atmospheric dielectric barrier discharge plasma treatment *PLoS One* **8** e82143

[44] Eisenhauer P, Chernets N, Song Y, Dobrynin D, Pleshko N, Steinbeck M J and Freeman T A 2016 Chemical modification of extracellular matrix by cold atmospheric plasma-generated reactive species affects chondrogenesis and bone formation *J. Tissue Eng. Regen. Med.* **10** 772–82

[45] Przekora A and Ginalska G 2015 Enhanced differentiation of osteoblastic cells on novel chitosan/β-1,3-glucan/bioceramic scaffolds for bone tissue regeneration *Biomed. Mater.* **10** 015009

[46] Przekora A and Ginalska G 2017 Chitosan/β-1,3-glucan/hydroxyapatite bone scaffold enhances osteogenic differentiation through TNF-α-mediated mechanism *Mater. Sci. Eng.* C **73** 225–33

[47] Neve A, Corrado A and Cantatore F P 2011 Osteoblast physiology in normal and pathological conditions *Cell Tissue Res.* **343** 289–302